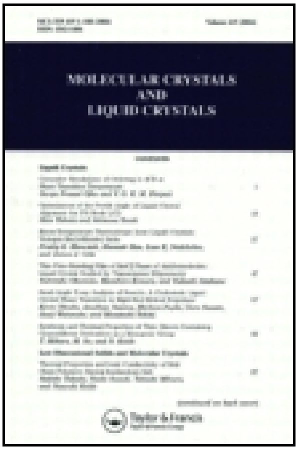

Molecular Crystals and Liquid Crystals
Publication details, including instructions for authors and subscription information:
http://www.tandfonline.com/loi/gmcl20

Spin density wave with a reduced anisotropy in (TMTSF) 2 PF 6

Keizo Murata [a] , Yoshiyuki Mizuno [a] , Fan Zhung Guo [a] , Sadayuki Shodai [a] , Ken-Ichi Iwashita [a] & Harukazu Yoshino [a]

[a] Department of Material Science, Graduate School of Science, Osaka City University, Sumiyoshi-ku, Osaka-shi, 558-8585, Japan

Version of record first published: 18 Oct 2010

Mol. Cryst. Liq. Cryst., Vol. 380, pp. 85-92

1058-725X/02 \$12.00 + .00
DOI: 10.1080/10587250290101405

SPIN DENSITY WAVE WITH A REDUCED ANISOTROPY IN $(TMTSF)_2PF_6$

Keizo Murata, Yoshiyuki Mizuno, Fan Zhung Guo, Sadayuki Shodai, Ken-Ichi Iwashita and Harukazu Yoshino
Department of Material Science, Graduate School of Science, Osaka City University, Sumiyoshi-ku, Osaka-shi 558-8585, Japan

The temperature-uniaxial pressure (T-P) phase diagram of metal, spin density wave in $(TMTSF)_2PF_6$ was apparently quite similar to that of hydrostatic pressure irrespective of the direction of the uniaxial pressure in strain method. However, by the examination of ρ_a, $\rho_b{}'$ and $\rho_c{}^*$ under three uniaxial pressures, it was found that the new phase diagram is based on quite different electronic structure among three uniaxial pressures. The reduction SDW by a-compression must primarily be due to the reduction of density of state, with which electron correlation is important. The strain along b' and c^*-axes reduces strongly the anisotropy, i.e. $t_a/t_{b'} = 4.3$ with $p//c^* = 10$ kbar, for instance, where still SDW is present.

Keywords: TMTSF; $(TMTSF)_2PF_6$; uniaxial pressure; uniaxial strain; electronic properties; anisotropy; spin density wave; Fermi surface nesting; electron correlation

1. INTRODUCTION

The temperature-pressure (T-P) phase diagram of metal, spin density wave (SDW) and superconductivity in $(TMTSF)_2PF_6$ is already widely known [1]. The suppression of SDW by pressure is commonly explained by reducing the nesting of the quasi-one-dimensional (Q1D) Fermi surface, whose 1D band is basically expressed as,

$$\varepsilon(\boldsymbol{k}) = -2t_a \cos(k_a a) - 2t_b \cos(k_b b) - 2t_c \cos(k_c c) \tag{1}$$

where t_a, t_b and t_c are the transfer energies along three directions, with 2000 K, 200 K, 7 K, respectively. Compared with hydrostatic pressure, the method of uniaxial pressure allows more independent control of t_a, t_b, t_{c^*} or

This work was carried out as a part of 'Research for the Future' project, JSPS-RFTF97P00105, supported by Japan Society for the Promotion of Science.

taking account of the triclinicity, t_a, $t_{b'}$ or t_{c*}. Therefore, it is quite suitable to apply this method to *control* SDW to understand this instability more precisely. The parameter, ${t_b}^2/t_a$ is a good measure for considering nesting. And a perfect nesting is realized when ${t_b}^2/t_a = 0$, which gives the highest T_{SDW}.

Historically, the method of uniaxial pressure was applied to the study of organic conductors by Campos et al., by compressing the sample together with epoxy, which was called "uniaxial stress method" [2]. However, the uniaxial stress method accompanies an expansion along the other two axes as is characterized by Poisson's ratio. It is then refined to a "uniaxial strain method" by Maesato et al. [3], which does not allow the expansion to two other directions, since this method adopts the rigid pressure cell which has been used for hydrostatic pressure. This is called uniaxial strain method and is expected to be more ideal way of changing the transfer energies independently [4]. Further, this technique allows to achieve much higher pressure than the stress technique.

Figure 1 shows a *T-P* (uniaxial) phase diagram of $(TMTSF)_2PF_6$ obtained by the resistance measurement [5]. Before starting this work, we expected that the strain along the 1-D axis, which we call "a-strain" here, would give rise to a better nesting and would enhance T_{SDW}. In the same way, we expected "b'-strain" suppressed SDW. Against these expectations, strain along all three directions suppressed SDW, as shown in Figure 1. Rather, a-strain was most effective, then b'- and c*-strains followed. Further remarkable result was that the effect of strain was almost the same among those of three directions, and even with that of hydrostatic pressure. We were very much interested in the origin of this result. The purpose of this paper is to show that this new *T-P* (uniaxial) phase diagram is

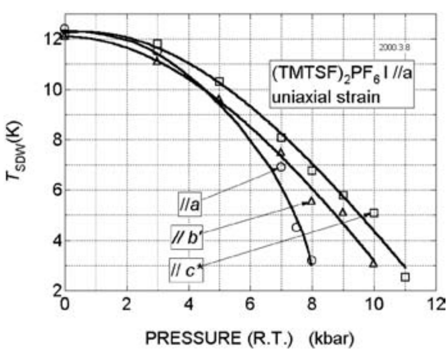

FIGURE 1 Variation of T_{SDW} against the uniaxial pressure in the strain method. Pressure values are at room temperature in unit of kbar. The actual low temperature pressure is expected to be smaller by 1–1.5 kbar.

originated from the electronic structure quite different from that of the naturally grown crystal anisotropy of $(TMTSF)_2PF_6$. In this work, we concentrated our work on the anisotropy under uniaxial pressure by conductivity measurement along three directions, i.e. nine combinations of anisotropy study.

2. EXPERIMENT

As described in the previous paper [5], the procedure of the measurement was the following. Four terminal electrical contacts were made on samples with carbon paste (XC-12) with gold wires. Then, to protect the sample against the epoxy (Stycast 1266) and its hardener, samples were thinly covered with GE7031 varnish. Then the samples were buried in the precured epoxy, which was then hardened. Usually, two or three samples were prepared in the same cell to obtain the reproducibility. In the separate run, we confirmed by strain gauge that the strain is actually generated uniaxially in the sample environment with epoxy but hydrostatically[5] with Daphne 7373 oil.*

3. EXPERIMENTAL RESULTS

In order to estimate the transfer energies, we studied ρ_{a}, $\rho_{\mathrm{b'}}$ and $\rho_{\mathrm{c^*}}$ independently under uniaxial strain configurations along a-, b'- and c^*, respectively. Figures 2–4 show normalized resistance under these configurations of strain. In the following we list features of these results.

i) The variation in resistance against the a-strain is almost the same as that under hydrostatic pressure.
ii) The variation of ρ_{a}, $\rho_{\mathrm{b'}}$ and $\rho_{\mathrm{c^*}}$ against the a-strain seems to be scaled, while two other strains cause differently to the variation of ρ_{a}, $\rho_{\mathrm{b'}}$ and $\rho_{\mathrm{c^*}}$.
iii) The vertical scale in Figure 2 is linear, while logarithmic scales were required to show the results in Figures 3 and 4. In other words, the resistivity decrease in Figures 3 and 4 by 3–4 orders of magnitude is extremely large, which has never been observed as far as we know or at least in organic conductors, except in the case of occurrence of phase transition.

*It might be worth noted that compressing beyond the solidification pressure inevitably induced uniaxial component. The mixture of Fluorinate 70 and 77 for example solidifies at 1 GPa at room temperature. Compared with that, Daphne 7373 does not solidify at room temperature in the usual working pressure of organic conductors [6].

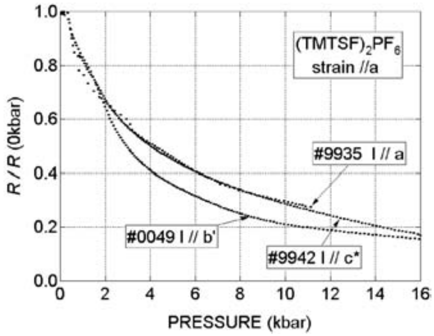

FIGURE 2 Normalized resistivity by the uniaxial pressure by strain method along the a-axis.

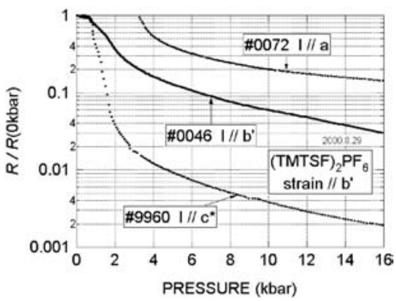

FIGURE 3 The same as Figure 2 but with strain along the b'-axis. *Three* span logarithmic scale is used for vertical scale.

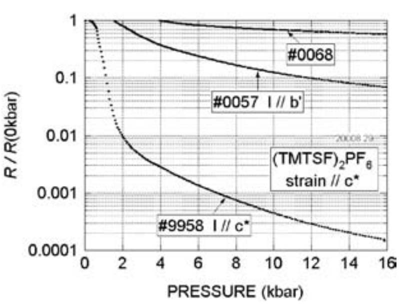

FIGURE 4 The same as Figure 2 but with strain along the c*-axis. *Four* span logarithmic scale is used for vertical scale.

From these features, it is clear that the new *T-P*(uniaxial) phase diagram as shown in Figure 1 is *based on completely different* anisotropy or electronic structure, in spite of the apparent similarity in the *T-P* phase diagram among the three uniaxial pressures and even between the hydrostatic pressure.

4. DISCUSSION

We can interpret the fact i) in Sec. 3 in the following way. In the case of hydrostatic pressure, according to Morosin [7], the a-axis is the most compressive, and then the b- and c-axes, i.e. $-d\ln x/dP(\%\text{kbar}) = 0.46(3)$, 0.08(5), and 0.01(6), where x is a, b and c, respectively. Therefore, the effect of uniaxial pressure may result similarly to that of hydrostatic pressure.

The scaling behavior mentioned above in ii) implies that the effect of a-strain is governed by a single parameter. And we expect that this parameter also rule the suppression of SDW or T_{SDW} itself. The ruling parameter for SDW is nesting, density of states, $N(0)$ and on-site Coulomb energy, U. When we consider nesting, denesting parameter appears as a second harmonics of t_{b} term in Eq. (1), as $t_{\mathrm{b}}'\cos(2k_{\mathrm{b}}b)$ when k_{a} component is linearized. The value of t_{b}' is expressed as $t_{\mathrm{b}}{}^2\cos(ak_{\mathrm{F}})/4t_{\mathrm{a}}\sin^2(ak_{\mathrm{F}})$. With this expression of t_{b}', we expected that a-strain improved nesting, which gives rise to T_{SDW} but which is against the experimental fact as shown in Figure 1. To solve this problem, we proposed the possibility of enhancement of t_{b} by a-strain. The real system is triclinic and t_{b} is consisted of more than one transfer energies [1], which can be enhanced by the shrinkage along the a-axis [5].

Miyazaki et al. evaluated the effect of the a-strain to the degree of nesting and T_{SDW}. Their calculated result shows the improvement of nesting but at the same time the reduction of density of state is not negligible, which overwhelms the improvement of nesting [8]. The reduction of density of states may explain the scaled behavior of ii). Since the density of state appears as $\exp(-UN(0))$, the Coulomb correlation is to be taken into account.

In their paper, the improvement of nesting is shown as the decrease of t_{b} and with the increase of t_{a}. This is not consistent with our speculation that the anisotropy of $t_{\mathrm{b}}/t_{\mathrm{a}}$ is constant with a-strain. This is an interesting subject to be solved in the future.

We next discuss about the strong reduction of resistivity $\rho_{\mathrm{b}'}$ and ρ_{c^*} under uniaxial pressure by b'- and c^*-strains, which was summarized above as iii). These enormous reduction in resistivity directly results in the remarkable reduction in anisotropy. Based on the results of Figures 2–4, we

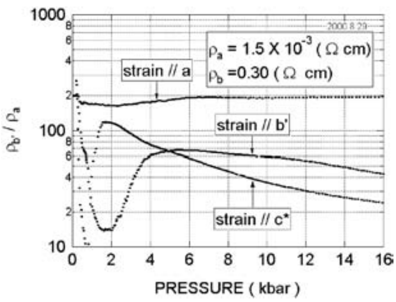

FIGURE 5 Uniaxial pressure dependence of $\rho_{b'}/\rho_a$ of $(TMTSF)_2PF_6$ at room temperature. *Three* span logarithmic scale is used for vertical scale.

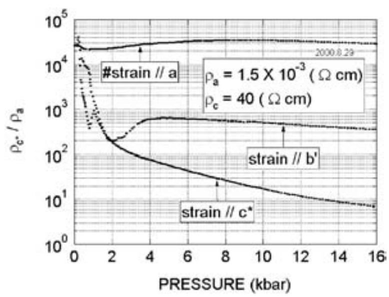

FIGURE 6 Uniaxial pressure dependence of ρ_{c*}/ρ_a of $(TMTSF)_2PF_6$ at room temperature. *Four* span logarithmic scale is used for vertical scale.

show $\rho_{b'}/\rho_a$ and ρ_{c*}/ρ_a in Figures 5 and 6, respectively, as a function of uniaxial pressures.

From these data, we can estimate how the ratio, $t_a/t_{b'}$ varies against the b'-strain (or c*-strain) at room temperature. The ratio, $\rho_{b'}/\rho_a$ reduced from 200 for $p = 0$ to 60 (or 37) for 10 kb of $//b'$-strain (or of c*-strain). Considering the relation, $(\rho_{b'}/\rho_a)^{1/2} \propto t_a/t_{b'}$ the ratio $t_a/t_{b'}$ must have changed from 10 ($=2000\,K/200\,K$) for $p = 0$ to 5.5 (or 4.3) for 10 kb of b'-strain (or of c*-strain), close to which SDW is still present.

The similar calculation was carried out for ρ_{c*}/ρ_a, which changed from 2.7×10^4 for $p = 0$ to 4.4×10^2 (or 12) for 12 kb of b'-strain (or c*-strain). With the same estimation, the ratio t_a/t_{c*} must have changed from 285 ($=2000\,K/7\,K$) for $p = 0$ to 36 (or 6.0) for 12 kb of b'-strain (or c*-strain).

Therefore compared with that of a-strain where anisotropy is unchanged, the effect of b'- and c*-strains to SDW is actually by a strong reduction of anisotropy. But what is remarkable is that the effect to reduce

SDW is almost the same among the strains of the three directions or even the strongest with a-strain.

As discussed above, t_b/t_a increases from $0.1(=1/10)$ to $0.18\ (=1/5.5)$ for b'-strain $=10$ kb, up to which SDW is present. Although we can only discuss the ratio of transfer energies by the present experiment, as a comparison, in the theory of Yamaji,[1] SDW should be suppressed by 50% increase in t_b from 200 K.

What happens with the electron correlation, density of states in the case of b'- and c^*-strains, is an interesting subject, but is left in the future.

Essentially the density of state and Fermi surface nesting are related to band parameters. With this motivation, we started transport experiment in high magnetic field in Tallahassee and Tsukuba, in collaboration with Brooks and Uji. Preliminary results on the new electronic structure realized under c^*-strain are about the rapid oscillation and field induced SDW. Rapid oscillation is observed only below 6 kbar, and FISDW is only 14 kbar but not at 11 kbar. (Pressures are the values of room temperature, at low temperature, 1–1.5 kbar pressure loss is expected.) Details will be presented elsewhere.

CONCLUSION

We examined uniaxial pressure (//a, //b′ and //c*) dependence of ρ_a, $\rho_{b'}$ and ρ_{c^*}. It was found that although the temperature-uniaxial pressure (T-P) phase diagram of metal, spin density wave in (TMTSF)$_2$PF$_6$ was apparently quite similar to that of hydrostatic pressure irrespective of the direction of the uniaxial pressure in strain method, those phase diagrams were found to be based on quite different anisotropy or electronic structure. The a-strain did not change anisotropy, (which is not consistent with the model of Miyazaki), while other strains reduced enormously the anisotropy. Comparing the effect of a-strain and that of others, at least the primary effect of a-strain to the suppression of SDW must be due the reduction of the density of state, this means that electron correlation is important. The effect of other strains reduce enormously the anisotropy, i.e. $t_a/t_{b'}=4.3$ at $p//c^*=10$ kbar, for instance, however, it is noted that SDW is still present.

REFERENCES

[1] Ishiguro, T., Yamaji, K., & Saito, G. (1998). *Organic Superconductors*, Springer, Berlin.

[2] Campos, C. E., Brooks, J. S., van Bentum, P. J. M., Perenboom, J. A. A., Klepper, S. J., Sandhu, P. S., Valfells, S., Tanaka, Y., Kinoshita, T., Kinoshita, N., Tokumoto, M., & Anzai, H. (1996). *Rev. Sci. Instrum*, *66*, 1061 (1995), and *Phys. Rev. B 52*, R7014.

[3] Maesato, M., Kaga, Y., Kondo, R., & Kagoshima, S. (2000). *Rev. Sci. Instrum.*, *71*, 176.
[4] Kagoshima, S., these proceedings.
[5] Guo, F. Z., Murata, K., Oda, A., Mizuno, Y., & Yoshino, H. (2000). *J. Phys. Soc. Jpn.*, *69*, 2164.
[6] Kagayama, T., private communications.
[7] Morosin, B., Schirber, J. E., Greene, R. L., & Engler, E. M. (1982). *Phys. Rev.*, *B 26*, 2660.
[8] Miyazaki, M., Kishigi, K., & Hasegawa, Y. (2000). *J. Phys. Soc. Jpn.*, *69*, 997.